Eur. J. Mineral.
2006, **18**, 175–186

Thermodynamic properties and crystal structure refinement of ferricopiapite, coquimbite, rhomboclase, and $Fe_2(SO_4)_3(H_2O)_5$

JURAJ MAJZLAN[1,2,*], ALEXANDRA NAVROTSKY[2], R. BLAINE MCCLESKEY[3] and CHARLES N. ALPERS[4]

[1]Institute of Mineralogy, Petrology and Geochemistry, Albert-Ludwig-University of Freiburg, Albertstraße 23b, D-79104 Freiburg, Germany
*Corresponding author, e-mail: Juraj.Majzlan@minpet.uni-freiburg.de
[2]Thermochemistry Facility and Department of Geology, University of California at Davis, Davis CA 95616, USA
[3]U.S. Geological Survey, 3215 Marine Street, Suite E-127, Boulder CO 80303, USA
[4]U.S. Geological Survey, 6000 J Street, Placer Hall, Sacramento CA 95819, USA

Abstract: Enthalpies of formation of ferricopiapite [nominally $Fe_{4.67}(SO_4)_6(OH)_2(H_2O)_{20}$], coquimbite [$Fe_2(SO_4)_3(H_2O)_9$], rhomboclase [$(H_3O)Fe(SO_4)_2(H_2O)_3$], and $Fe_2(SO_4)_3(H_2O)_5$ were measured by acid (5 N HCl) solution calorimetry. The samples were characterized by wet chemical analyses and synchrotron powder X-ray diffraction (XRD). The refinement of XRD patterns gave lattice parameters, atomic positions, thermal factors, and occupancies of the sites. The calculated formulae differ slightly from the nominal compositions: $Fe_{4.78}(SO_4)_6\ (OH)_{2.34}(H_2O)_{20.71}$ (ferricopiapite), $(Fe_{1.47}Al_{0.53})(SO_4)_3(H_2O)_{9.65}$ (coquimbite), $(H_3O)_{1.34}Fe(SO_4)_{2.17}(H_2O)_{3.06}$ (rhomboclase), and $Fe_2(SO_4)_3(H_2O)_{5.03}$. All thermodynamic data are given per mole of these formulae.

The measured standard enthalpies (in kJ/mol) of formation from the elements (crystalline Fe, Al, S, and ideal gases O_2 and H_2) at T = 298.15 K are –4115.8±4.1 [$Fe_2(SO_4)_3(H_2O)_{5.03}$], –12045.1±9.2 (ferricopiapite), –5738.4±3.3 (coquimbite), and –3201.1±2.6 (rhomboclase). Standard entropy (S^o) was estimated as a sum of entropies of oxide, hydroxide, and sulfate components. The estimated S^o (in J/mol·K) values for the iron sulfates are 488.2 [$Fe_2(SO_4)_3(H_2O)_{5.03}$], 1449.2 (ferricopiapite), 638.3 (coquimbite), and 380.1 (rhomboclase). The calculated Gibbs free energies of formation (in kJ/mol) are –3499.7±4.2 [$Fe_2(SO_4)_3(H_2O)_{5.03}$], –10089.8±9.3 (ferricopiapite), –4845.6±3.3 (coquimbite), and –2688.0±2.7 (rhomboclase). These results combined with other available thermodynamic data allow construction of mineral stability diagrams in the $Fe^{III}_2(SO_4)_3$–$Fe^{II}SO_4$–H_2O system. One such diagram is provided, indicating that the order of stability of ferric sulfate minerals with decreasing pH in the range of 1.5 to –0.5 is: hydronium jarosite, ferricopiapite, and rhomboclase.

Key-words: copiapite, coquimbite, rhomboclase, sulfate minerals, thermodynamics, crystal structure.

Introduction

The exploitation of mineral resources has increased steadily over the past several decades, resulting in ever-larger production of mining waste (*e.g.*, Young, 1992). Mining and mineral processing operations commonly result in environmental effects that may persist for decades to centuries after the operations have ceased. Although the waste handling practices are continuously improving, environmental problems that need to be addressed remain in abundance. A well known, widespread problem linked to the mining and processing of sulfide-bearing metal ores and coal is acidic drainage. The acidic waters usually originate because of previous or current mining activity, more rarely from purely natural sources.

Acidic drainage is caused by the oxidation of sulfide minerals (most commonly pyrite, marcasite, or pyrrhotite) and the subsequent aqueous transport of soluble reaction products. The dominant oxidants are atmospheric oxygen (usually in the form of dissolved oxygen in water) and dissolved ferric iron (Nordstrom & Alpers, 1999a). Pyrite (FeS_2) is the most common sulfide mineral in the Earth's crust and its oxidation, commonly mediated by microbes, is the primary cause of acidic drainage. Reaction products of pyrite oxidation are sulfuric acid and dissolved iron, both ferrous and ferric. The resulting sulfuric acid solutions attack other sulfides and rock-forming minerals resulting in acidic waters that typically contain elevated concentrations of trace metals (*e.g.*, Al, Cu, Cd, and Zn) that are toxic to aquatic life and humans. Precipitation of efflorescent metal salts from acidic waters occurs in response to changes in temperature, pH, oxidation of ferrous iron, and evaporation (Nordstrom & Alpers, 1999a). One important category of the efflorescent salts commonly formed from acidic waters is hydrated ferric sulfate minerals (Jambor *et al.*, 2000; Jambor, 2003; Jerz & Rimstidt, 2003), the subject of this study. Ferric sulfate minerals are important in the environment because they store metals and acidity in a highly soluble form that can be readi-

0935-1221/06/0018-0175 $ 5.40
DOI: 10.1127/0935-1221/2006/0018-0175

ly released during wet conditions. The release of ferric iron stored in ferric sulfate minerals can stimulate continued sulfide oxidation in ground waters even in the absence of dissolved oxygen, which can confound expected benefits of mine plugging as a means of preventing the formation of additional acidic drainage (*e.g.*, Cravotta, 1994; Alpers *et al.*, 2003).

Thermodynamic data for the Fe^{III} sulfates are needed to evaluate the role of these minerals in acidic waters and to model reaction paths. With the exception of recent estimates by Hemingway *et al.* (2002), no thermodynamic data are available for Fe^{III} sulfates such as coquimbite or ferricopiapite.

In this paper, we report measurements of formation enthalpy of $Fe_2(SO_4)_3(H_2O)_5$, ferricopiapite [nominally $Fe_{4.67}(SO_4)_6(OH)_2(H_2O)_{20}$], coquimbite [$Fe_2(SO_4)_3(H_2O)_9$], and rhomboclase [$(H_3O)Fe(SO_4)_2(H_2O)_3$]. The phase $Fe_2(SO_4)_3(H_2O)_5$ was included in the study despite the fact that it is not a mineral. At the time when the calorimetric experiments were performed, we assumed that this phase is identical with the mineral lausenite. Later investigation (Majzlan *et al.*, 2005a) showed that the relationship is not straightforward. Yet, because the studied phase belongs to the chemical system under investigation, we decided to present the data for $Fe_2(SO_4)_3(H_2O)_5$ in this work. Synthetic materials were used for all compounds with the exception of coquimbite, for which a natural specimen was used. Each phase was characterized by wet chemical analysis and powder X-ray diffraction, with both conventional Cu Kα source and a tunable source at a synchrotron. We then estimated the standard entropy of these sulfates to calculate their Gibbs free energy of formation. This contribution should be regarded as incremental progress toward a more complete thermodynamic description of sulfate mineral assemblages in acidic drainage environments. Significant gaps remain in our understanding of these systems, such as thermodynamic data for most Fe^{III} and mixed Fe^{II}-Fe^{III} sulfates. Specific ion interaction models of concentrated Fe^{III}- and mixed Fe^{II}-Fe^{III} sulfate solutions have long been needed (Ptacek & Blowes, 2000) and appeared only very recently (Christov, 2004; Rumyantsev *et al.*, 2004). One of the reasons why the thermodynamic modeling of acidic waters is difficult is the high ionic strength of the fluid phase. The data presented in this paper, together with ion-interaction models for the fluids associated with these phases (cited above), are steps toward addressing these problems. A comprehensive thermodynamic model of water-mineral reactions in low-temperature acid-sulfate systems remains a future goal. In this sense, our cumulative understanding of sulfate mineral systems and associated waters is still limited compared with other rock-forming mineral groups such as silicates, oxides, and carbonates.

Materials and methods

In addition to the title compounds, several other phases had to be synthesized for the calorimetric experiments. These are α-$MgSO_4$, $Al_2(SO_4)_3$, γ-FeOOH, and MgO. The reason why these phases had to be included in the set of studied compounds is explained in the section "Thermodynamics of the reference materials" below.

For the syntheses of the hydrated ferric sulfates, sulfuric acid, deionized water, and ferric sulfate were the starting compounds. Sulfuric acid was 96 % H_2SO_4 by mass, with density of 1.84 g/cm^3. Two batches of ferric sulfate were received from the supplier (Alfa Aesar), both labeled as $Fe_2(SO_4)_3(H_2O)_x$. The first batch was a fine-grained, homogeneous, pale brown powder that contained ~21 % water and was X-ray amorphous. The second batch was coarser, yellow, with occasional brownish or white grains, and contained ~28 % water. According to XRD analysis, it was composed of a copiapite-group mineral and a minor amount of kornelite [$Fe_2(SO_4)_3(H_2O)_{7.25}$]. In the following description, ferric sulfate will refer to the first $Fe_2(SO_4)_3(H_2O)_x$ batch. Although both batches came from the same supplier, under the same description, not all syntheses could be achieved using the second batch. This discrepancy was probably due to its coarser grain size and sluggish dissolution in water. The starting compositions for the mixtures of sulfuric acid, water, and ferric sulfate were taken from the phase diagrams of Posnjak & Merwin (1922). In all cases, the phase precipitating from the solution was found to be the phase determined by Posnjak & Merwin (1922).

Rhomboclase precipitated from a solution made of 2.5 g of ferric sulfate, 5 mL of water, and 1.36 mL of sulfuric acid. The solution was allowed to evaporate slowly at room temperature, turning into a pale yellow mass of the product.

Ferricopiapite was synthesized by mixing 1.17 mL of water and 2.5 g of ferric sulfate. The solid dissolved completely in water after ~30 min in an ultrasonic bath. The solution was sealed in a silica-glass capsule and kept at 323 K. Yellow precipitate appeared after 2 days and slowly grew in volume for the following 7 days. Afterwards, the capsule was open, the product washed with ethanol and dried at room temperature by filtering under reduced pressure.

$Fe_2(SO_4)_3(H_2O)_5$ was prepared by mixing 1.52 mL water, 0.48 mL of sulfuric acid, and 1.98 g of ferric sulfate. The mixture was sealed in a silica glass capsule and left in an oven at 403 K. After four days, the capsule was allowed to cool to 363 K, broken, and the precipitate was filtered under reduced pressure and washed several times with ethanol, and dried at 323 K.

The coquimbite sample was picked from a large (2 × 2 × 2 cm), compact aggregate of pinkish coquimbite from the Richmond mine at Iron Mountain, near Redding, California (Nordstrom & Alpers, 1999b; Alpers *et al.,* 2003). The aggregate was overgrown at a few spots by copiapite and voltaite, and care was taken to avoid contamination of the sample by these minerals.

The low temperature polymorph of $MgSO_4$ (α-$MgSO_4$) was synthesized by the method outlined by Ko & Daut (1980). Two grams of $MgSO_4(H_2O)_{\sim 7}$ (Alfa Aesar, reagent grade) were ground and heated at 423 K in a platinum crucible for 2 hours. The crucible was then withdrawn from the furnace, the powder quickly disintegrated and mixed thoroughly with 0.5 mL of concentrated sulfuric acid. The furnace was set at 588 K and the powder was heated for 24 hours. The mixing with sulfuric acid and 24 h heating at 588 K was repeated once more. Because anhydrous $MgSO_4$ is

strongly hygroscopic, the sample was withdrawn from the furnace, quickly transferred, allowed to cool, and later handled in a glove box with argon atmosphere (< 1 ppm H_2O).

MgO (Alfa Aesar, 99.99 % metals basis) was heated at 1800 K overnight in a platinum crucible. For the duration of the experiments, the sample was kept at 1200 K in a Pt crucible in a muffle furnace. The sample was withdrawn from the furnace for each experiment; the required amount to be used in calorimetry was removed, and the sample was returned to the furnace.

Anhydrous $Al_2(SO_4)_3$ (synthetic millosevichite) was prepared by heating $Al_2(SO_4)_3(H_2O)_{\sim 18}$ (reagent grade, Alfa Aesar) in a Pt crucible at 723 K for 4 hours. The sample was then allowed to cool, stored and handled in a glove box with argon atmosphere.

The γ-FeOOH sample was previously synthesized and characterized by Majzlan *et al.* (2003). The same sample that was used in that investigation was also used here.

Conventional powder X-ray diffraction (XRD) patterns of all samples were collected with a Scintag PAD V diffractometer with Cu Kα radiation and a diffracted-beam graphite monochromator. The patterns were collected in the range 5–60 °2Θ, with a step of 0.02 °2Θ and dwell of 8 s at each step. Lattice parameters were calculated by profile fit using GSAS (Larson & von Dreele, 1994). The performance of the diffractometer was regularly checked by collecting an XRD pattern of LaB_6 (NIST standard reference material 660) or Si (NIST standard reference material 640). The lattice parameters determined for LaB_6 or Si in our laboratory were always found to be within ±0.0004 Å from the certified values.

Synchrotron powder XRD patterns of the ferric sulfates were collected at the bending magnet beamline X3B1 at National Synchrotron Light Source (Brookhaven National Laboratory). X-rays with a wavelength of 1.14959(1) Å were selected using a double crystal Si(111) monochromator. The wavelength and the zero angle of the diffractometer were determined with a NIST standard reference material 1976 (corundum, α-Al_2O_3). Samples were loaded into 1.0 mm glass capillary tubes. The intensity of the incoming beam was monitored during data collection by an ion chamber and the measured intensities of the diffracted beam were normalized (corrected) for the decay of the primary beam. The diffracted beam was analyzed by a Ge(111) crystal and Na(Tl)I scintillation detector. The XRD patterns were collected at room temperature, over angular range of 3 or 6.5 (depending on the position of the first peak) to 60 °2Θ, step of 0.005 °2Θ, and dwell of 2 s. The refined structural parameters are reported in Tables 1–4. Numbers in parentheses in these tables are the statistical estimated standard deviations on the last digit from the Rietveld refinement, and are substantially smaller than any realistic estimate of accuracy. The real magnitude of errors in the Rietveld refinement is much more difficult to ascertain (see Young, 1993).

Table 1. Lattice parameters (Å, °) of the phases used in this study. For the Fe^{III} sulfates, the parameters were determined from synchrotron XRD. For the other phases, they were determined from conventional XRD experiments. All values were determined by Rietveld refinement, using starting model from the references listed. The lattice parameters from the starting models are given for comparison.

phase	space group	lattice parameters (our samples)	starting model for the Rietveld refinement	lattice parameters (in the starting model)
α-$MgSO_4$	*Cmcm*	*a* = 5.1714(3) *b* = 7.8720(4) *c* = 6.4850(4)	Rentzeperis & Soldatos (1958)	*a* = 5.182(15) *b* = 7.893(2) *c* = 6.506(16)
ferricopiapite	$P\bar{1}$	*a* = 7.3867(6) *b* = 18.363(2) *c* = 7.3275(5) α = 93.940(5) β = 102.201(5) γ = 98.916(4)	Fanfani *et al.* (1973)	*a* = 7.390(8) *b* = 18.213(10) *c* = 7.290(8) α = 93.67(25) β = 102.05(42) γ = 99.27(25)
coquimbite	$P\bar{3}1c$	*a* = 10.9153(4) *c* = 17.0770(8)	Fang & Robinson (1970)	*a* = 10.922(9) *c* = 17.084(14)
$Fe_2(SO_4)_3(H_2O)_{5.03}$	$P2_1/m$	*a* = 10.705(1) *b* = 11.080(1) *c* = 5.574(1) β = 98.864(6)	Majzlan *et al.* (2005a)	*a* = 10.679(2) *b* = 11.053(3) *c* = 5.567(1) β = 98.89(1)
lepidocrocite	$Cmc2_1$	*a* = 3.0680(2) *b* = 12.5270(9) *c* = 3.8699(2)	Christensen & Christensen (1978)	*a* = 3.08(1) *b* = 12.50(1) *c* = 3.87(1)
millosevichite	$R\bar{3}$	*a* = 8.057(2) *c* = 21.246(6)	Dahmen & Gruehn (1993)	*a* = 8.0246(4) *c* = 21.3570(10)
periclase	*Fm3m*	*a* = 4.2110(1)	Tsirelson *et al.* (1998)	*a* = 4.214(1)
rhomboclase	*Pnma*	*a* = 9.7226(8) *b* = 18.2800(9) *c* = 5.4270(5)	Mereiter (1974)	*a* = 9.724(4) *b* = 18.3330(90) *c* = 5.421(4)

Table 2. Fractional atomic coordinates and isotropic displacement parameters (in Å^2) for rhomboclase. Occupancy of the sites is 1 unless noted otherwise. Space group and lattice parameters are given in Table 1.

	Wyckoff position	*x*	*y*	*z*	U_i*100	occ
Fe1	4*a*	0	0	0	2.96(6)	
S1	8*d*	0.2375(3)	0.0868(1)	0.2849(5)	3.30(8)	
O1	8*d*	0.3264(5)	0.0217(3)	0.343(1)	4.46(9)	
O2	8*d*	0.0932(5)	0.0557(3)	0.253(1)	4.46(9)	
O3	8*d*	0.2881(6)	0.1203(3)	0.063(1)	4.46(9)	
O4	8*d*	0.2269(6)	0.1329(3)	0.505(1)	4.46(9)	
O5	8*d*	0.4884(7)	0.0869(3)	0.733(1)	4.46(9)	
O6	4*c*	0.6318(9)	1/4	0.550(2)	4.46(9)	
O7	4*c*	0.3916(10)	1/4	0.584(2)	4.46(9)	0.895(7)
O8	4*c*	0.428(8)	1/4	0.141(13)	4.46(9)	0.105(7)

Table 3. Fractional atomic coordinates and isotropic displacement parameters (in Å^2) for ferricopiapite. Occupancy of the sites is 1 unless noted otherwise. Space group and lattice parameters are given in Table 1.

	Wyckoff position	*x*	*y*	*z*	U_i*100	occ
Fe1	1*a*	0	0	0	2.99(7)	0.619(4)
Fe2	2*i*	0.7852(4)	0.31526(2)	0.5522(4)	2.99(7)	
Fe3	2*i*	0.5975(4)	0.67010(2)	0.8063(4)	2.99(7)	
S1	2*i*	0.8347(8)	0.7377(3)	0.2221(7)	3.47(10)	
S2	2*i*	0.8202(7)	0.4161(3)	0.2173(8)	3.47(10)	
S3	2*i*	0.6417(7)	0.1943(3)	0.1948(7)	3.47(10)	
O1	2*i*	0.741(1)	0.6755(5)	0.076(1)	4.58(9)	
O2	2*i*	0.685(1)	0.7644(6)	0.302(1)	4.58(9)	
O3	2*i*	0.053(1)	0.2961(5)	0.626(1)	4.58(9)	
O4	2*i*	0.055(2)	0.2053(5)	0.856(1)	4.58(9)	
O5	2*i*	0.621(1)	0.3915(5)	0.114(1)	4.58(9)	
O6	2*i*	0.836(2)	0.4896(5)	0.323(1)	4.58(9)	
O7	2*i*	0.883(1)	0.3609(5)	0.342(1)	4.58(9)	
O8	2*i*	0.937(1)	0.4245(5)	0.081(1)	4.58(9)	
O9	2*i*	0.560(1)	0.1156(4)	0.167(2)	4.58(9)	
O10	2*i*	0.510(1)	0.7613(6)	0.869(2)	4.58(9)	
O11	2*i*	0.791(1)	0.2163(6)	0.091(1)	4.58(9)	
O12	2*i*	0.723(2)	0.2169(5)	0.402(1)	4.58(9)	
O13	2*i*	0.468(2)	0.6594(6)	0.543(2)	4.58(9)	
O14	2*i*	0.692(2)	0.2725(6)	0.764(1)	4.58(9)	
O15	2*i*	0.866(1)	0.4144(5)	0.722(2)	4.58(9)	
O16	2*i*	0.225(1)	0.9516(6)	0.080(2)	4.58(9)	
O17	2*i*	0.696(1)	0.5723(5)	0.758(1)	4.58(9)	
O18	2*i*	0.041(1)	0.9885(5)	0.737(1)	4.58(9)	
O19	2*i*	0.834(2)	0.7266(5)	0.731(1)	4.58(9)	
O20	2*i*	0.173(2)	0.0938(6)	0.061(1)	4.58(9)	
O21	2*i*	0.768(1)	0.9160(5)	0.444(1)	4.58(9)	
O22	2*i*	0.536(2)	0.5621(6)	0.284(1)	4.58(9)	
O23	2*i*	0.642(1)	0.0732(5)	0.593(1)	4.58(9)	

The parameters refined for each phase include scale factor, 2 profile parameters for a pseudo-Voigt function with correction for reflection asymmetry (Finger *et al.*, 1994) (profile function #3 in GSAS), 3 background parameters for a cosine Fourier series background function (background function #2 in GSAS), and variable number of parameters for the atomic positions, atomic displacement factors, and site occupancies. In the case of partially occupied sites, their total occupancy was always constrained to 1.00. Displacement parameters for atoms of one element were always constrained to be equal. The total number of refined parameters for each phase is given in Table 5. Soft restraints were applied for the S-O bond distance for all three phases. Prior to the refinement, the elevated background in the central portion of each pattern, owing to scattering from the glass capillary, was removed by fitting a series of line segments to the background and subtracting. In the early stages of the refinement, the diffractometer zero was refined and afterwards kept constant.

Metal concentrations in the ferric sulfate samples were determined by inductively-coupled plasma (ICP-OES)

Table 4. Fractional atomic coordinates and isotropic displacement parameters (in Å^2) for coquimbite. Occupancy of the sites is 1 unless noted otherwise. Space group and lattice parameters are given in Table 1.

	Wyckoff position	*x*	*y*	*z*	U_i*100	occ
Al1	2*b*	0	0	0	3.53(6)	0.914(8)
Fe1	2*b*	0	0	0	3.53(6)	0.086(8)
Fe2	2*c*	1/3	2/3	1/4	3.53(6)	
Fe3	4*f*	2/3	1/3	0.0033(1)	3.53(6)	0.928(8)
Al3	4*f*	2/3	1/3	0.0033(1)	3.53(6)	0.072(8)
S1	12*i*	0.2451(2)	0.4145(2)	0.1225(2)	3.39(7)	
O1	12*i*	0.3191(5)	0.3452(5)	0.0918(3)	4.01(7)	
O2	12*i*	0.1056(5)	0.3076(5)	0.1552(3)	4.01(7)	
O3	12*i*	0.2235(5)	0.4942(5)	0.0587(3)	4.01(7)	
O4	12*i*	0.3360(5)	0.5145(5)	0.1833(3)	4.01(7)	
O5	12*i*	0.1653(5)	0.0702(6)	0.0635(3)	4.01(7)	
O6	12*i*	0.4512(4)	0.1187(5)	0.2122(3)	4.01(7)	
O7	12*i*	0.5698(5)	0.1613(5)	0.0737(3)	4.01(7)	

spectrometry. The samples were also analyzed by the Ferro-Zine method for Fe^{II} (Stookey, 1970), and Fe^{III} was determined by difference between total Fe and Fe^{II}. Sulfate was analyzed by ion chromatography. The total volatile content of the samples was determined by weight difference before and after firing overnight at 1200 K. The fired product was analyzed by energy-dispersive analysis (EDS), using a FEI-30XsFEG scanning electron microscope.

A commercial IMC-4400 isothermal microcalorimeter (Calorimetry Sciences Corporation) was used for the acid-solution calorimetry. The samples were weighed on a semi-microbalance, pressed into a pellet, and dropped into the solvent. Twenty-five mL of 5 N HCl (standardized solution, Alfa Aesar) were contained in the sample teflon cup. The sample size was dictated by the requirement of the stoichiometry and the mass of MgO samples that was chosen to be 3.00 mg. The mass of the sample pellets ranged than between 12 and 18 mg, depending on the sample studied. The reference teflon cup was filled by 25 mL of water and kept in its position for the duration of the experiments. The liquid bath of the calorimeter (44 L) held the cups and the thermopiles precisely at 298.15 K; the temperature fluctuation of the calorimeter was less than ± 0.001 K. The measured heat effects ranged from 0.04 to 12.0 J. With the exception of $Fe_2(SO_4)_3(H_2O)_5$, which gave the smallest heat effects (0.04–0.06 J), all other measured values were larger than 0.5 J, in average 2.7 J. In an independent series of runs, we found that the calorimeter is capable of detecting heat effects as small as 0.02 J in this configuration. The calorimeter was calibrated by dissolving KCl (NIST standard reference material 1655) in deionized water.

Table 5. Statistics of the Rietveld refinement for the synchrotron data. The structure of $Fe_2(SO_4)_3(H_2O)_5$ was refined by Majzlan *et al.* (2005a) and the results are reported in that work.

	ferricopiapite	rhomboclase	coquimbite
χ^2	3.57	3.29	3.34
wR_p	0.126	0.135	0.119
number of data points	11419	11600	10699
number of refined parameters	101	38	36
minimum possible wR_p	0.0672	0.0752	0.0658

Results and discussion

All samples gave XRD patterns with sharp peaks. Conventional XRD experiments were used for initial phase identification, purity check, and lattice parameter determination. The purity of the reference phases was tested only by conventional XRD. The refined lattice parameters are given

Table 6. Bond distances in the studied Fe^{III} sulfates. The structure of $Fe_2(SO_4)_3(H_2O)_5$ was refined by Majzlan *et al.* (2005a) and the results are reported in that work.

coquimbite					
Al1/Fe1	O5 × 6	1.907(5)	S1	O1	1.453(7)
Fe2	O4 × 6	2.026(3)		O4	1.474(5)
Fe3/Al3	O3 × 3	1.962(5)		O3	1.486(6)
	O7 × 3	2.026(5)		O2	1.489(5)
rhomboclase					
Fe1	O1 × 2	1.933(5)	S1	O3	1.438(6)
	O2 × 2	1.935(6)		O4	1.463(6)
	O5 × 2	2.032(5)		O1	1.503(6)
				O2	1.523(6)
ferricopiapite					
Fe1	O26 × 2	1.94(1)	S4	O10	1.45(1)
	O22 × 2	2.00(1)		O9	1.48(1)
	O24 × 2	2.02(1)		O7	1.49(1)
Fe2	O18	1.986(9)		O8	1.49(1)
	O20	1.99(1)	S5	O14	1.45(1)
	O19	1.99(1)		O13	1.47(1)
	O13	2.02(1)		O12	1.48(1)
	O9	2.03(1)		O11	1.49(9)
	O21	2.065(9)	S6	O15	1.46(1)
Fe3	O16	1.95(1)		O17	1.49(1)
	O19	1.95(1)		O16	1.50(1)
	O7	2.02(1)		O18	1.51(1)
	O11	2.04(1)			
	O23	2.07(1)			
	O25	2.08(1)			

in Table 1. Synchrotron XRD patterns served also for refinement of atomic positions, site occupancies, and thermal factors for the ferric sulfates (Tables 2-4). Information about the statistical parameters describing the fits is presented in Table 5. Bond distances and angles are given in Tables 6 and 7, respectively. They compare well to previous work on these phases (see references in Table 1). The results of the structural analysis for $Fe_2(SO_4)_3(H_2O)_5$ are presented in a separate contribution (Majzlan *et al.*, 2005a). The conventional XRD patterns show no impurity peaks, either in the reference phases or in Fe^{III} sulfates. However, the synchrotron patterns of ferricopiapite and coquimbite indicate the presence of minor amounts of impurities. For the ferricopiapite sample, there is an impurity peak at d = 10.570 Å. For the coquimbite sample, there are peaks at d = 9.161, 4.056, and 3.292 Å that cannot be indexed in the hexagonal unit cell of this mineral. In either case, the peaks are much smaller than the peaks of the major phase in the same angular region, and we estimate that the impurity phases represent ≤ 1 % of the samples. Because the identity of the impurities is uncertain, we could not include them in the Rietveld refinement, and the estimate of their abundance is only crude.

There are partially occupied sites in all three Fe^{III} sulfates whose structures were analyzed by synchrotron XRD. In rhomboclase, one of the oxygen sites in the interlayer portion of the structure (see Mereiter, 1974) is disordered. Our results agree with single crystal study of Mereiter (1974) in terms of the relative occupancy of the two sites. However, the position of the oxygen on the site with lower occupancy is different in our results and in the data of Mereiter (1974). In ferricopiapite, it is the Fe1 site with occupancy of 0.619(4) (Table 3). Ideal occupancy of this site should be 2/3. Occupancy slightly lower than ideal was determined also by neutron diffraction for deuterated ferricopiapite (Majzlan & Kiefer, 2006) and it is not clear whether the discrepancy is an experimental artifact or another complication in the structure of ferricopiapite. In coquimbite, Fe and Al substitute for each other at sites (0,0,0) and (2/3,1/3,z) (Table 4). Aluminum has strong preference for the isolated (0,0,0) site coordinated by six H_2O molecules, while iron prefers the (2/3,1/3,z) site, coordinated by three oxygens (bridging oxygens to sulfur cations) and probably three water molecules.

Table 7. Bond angles in the studied Fe^{III} sulfates. The structure of $Fe_2(SO_4)_3(H_2O)_5$ was refined by Majzlan *et al.* (2005a) and the results are reported in that work.

coquimbite									
O1-S1	-O4	107.3(3)	O5-Al1	-O5	× 6	89.1(2)			
	-O3	109.4(3)			× 6	90.9(2)			
	-O2	110.2(4)	O4-Fe2	-O4	× 6	91.5(2)			
O2-S1	-O4	111.3(3)			× 3	89.5(2)			
	-O3	109.5(3)			× 3	87.5(2)			
O3-S1	-O4	109.2(3)	O3-Fe3	-O3	× 3	93.6(2)			
				-O7	× 3	91.8(2)			
					× 3	86.2(2)			
			O7-Fe3	-O7	× 3	88.4(2)			
rhomboclase									
O1-S1	-O2	105.0(3)	O1-Fe1	-O2	× 2	90.8(2)			
	-O3	108.4(3)			× 2	89.3(2)			
	-O4	109.1(3)	O1-Fe1	-O5	× 2	93.7(2)			
O2-S1	-O3	112.2(4)			× 2	86.3(2)			
	-O4	104.0(4)	O2-Fe1	-O5	× 2	86.9(2)			
O3-S1	-O4	117.4(3)			× 2	93.1(2)			
ferricopiapite									
O1-S1	-O2	107.0(7)	O18-Fe1	-O20	× 2	87.9(4)	O1-Fe3	-O5	86.7(4)
	-O3	105.5(6)			× 2	92.1(4)		-O10	89.0(4)
	-O4	110.7(6)	O16-Fe1	-O18	× 2	87.2(4)		-O17	87.3(4)
O2-S1	-O3	105.8(7)			× 2	92.8(4)		-O19	91.1(4)
	-O4	113.5(7)	O16-Fe1	-O20	× 2	93.4(5)	O5-Fe3	-O10	91.0(4)
O3-S1	-O4	113.8(6)			× 2	86.7(5)		-O13	93.8(5)
O5-S2	-O6	108.3(6)	O3-Fe2	-O7		81.9(4)		-O17	87.8(4)
	-O7	110.9(6)		-O12		87.0(4)	O10-Fe3	-O13	88.9(5)
	-O8	108.4(6)		-O14		97.9(4)		-O19	92.9(4)
O6-S2	-O7	112.0(6)		-O15		89.2(4)	O13-Fe3	-O17	88.9(4)
	-O8	108.4(6)	O7-Fe2	-O12		90.0(4)		-O19	88.2(5)
O7-S2	-O8	108.8(6)		-O13		91.6(5)	O17-Fe3	-O19	88.2(4)
O9-S3	-O10	109.4(6)		-O15		91.7(4)			
	-O11	115.3(6)	O12-Fe2	-O13		93.7(5)			
	-O12	109.0(6)		-O14		91.5(4)			
O10-S3	-O11	106.5(6)	O13-Fe2	-O14		88.6(5)			
	-O12	108.0(6)		-O15		90.3(4)			
O11-S3	-O12	108.5(6)	O14-Fe2	-O15		86.9(4)			

Table 8. Chemical analyses of the studied Fe sulfates, their formulae and molecular weight.

	$Fe_2(SO_4)_3(H_2O)_5$	ferricopiapite	coquimbite*	rhomboclase
wet chemical analysis				
Fe(total) (mg/kg)	226400	208300	145800	158400
Fe^{II} (mg/kg)	109	116	3	107
Fe^{III} (mg/kg)	226300	208200	145800	158400
Al (mg/kg)	n.a.	n.a.	20340	n.a.
SO_4 (mg/kg)	559700	449200	495000	591200
weight loss experiments				
weight loss (wt %)	67.44±0.10(6)	69.92±0.16(6)	73.84±0.11(7)	77.26±0.08(5)
initial weight (mg)	10.65–11.85	11.80–19.35	14.24–19.09	12.50–18.22
formula	$Fe_2(SO_4)_3(H_2O)_{5.03}$	$Fe_{4.78}(SO_4)_6$ $(OH)_{2.34}(H_2O)_{20.71}$	$(Fe_{1.47}Al_{0.53})(SO_4)_3$ $(H_2O)_{9.65}$	$(H_3O)_{1.34}Fe(SO_4)_{2.17}$ $(H_2O)_{3.06}$
M_r (g/mol)	490.50	1256.22	558.43	344.92

*for the concentration of minor and trace elements, see Table 9

Table 9. Concentration of minor and trace elements in the coquimbite sample. Major element concentration is given in Table 5. The concentration of any element listed does not exceed 0.01 atoms per formula unit of coquimbite in Table 8.

analyte	mg/kg	analyte	mg/kg	analyte	mg/kg
As	308	Cr	3	Ni	41
B	31	Cu	331	Pb	11
Ba	< 0.8	K	151	Si as SiO_2	< 56
Be	< 1	Li	< 2	Se	< 28
Ca	60	Mg	232	Sr	< 0.7
Cd	10	Mn	33	V	< 5
Co	6	Na	< 57	Zn	761

Our results agree very well with previous single crystal work of Fang & Robinson (1970).

Ferricopiapite, $Fe_2(SO_4)_3(H_2O)_5$, and rhomboclase were analyzed for Fe^{II}, total Fe, and SO_4 content (Table 8). Because of its natural origin, coquimbite was also analyzed for Al (Table 8) and a number of minor and trace elements (Table 9). None of these elements is present in a sufficient concentration to affect the results of the calorimetric measurements. The results of the weight-loss experiments (Table 8) give the total volatile content of the samples. EDS analyses of the products of the weight-loss experiments show only Fe (and Al for coquimbite), indicating that sulfur has been completely expelled from the samples upon heating.

The formulae used in the calorimetric cycle and thermodynamic analysis are based on the chemical analyses and weight loss experiments, and are constrained by the condition of charge balance. The chemical composition of the phase $Fe_2(SO_4)_3(H_2O)_5$ corresponds very closely to its nominal composition (Table 8; see also Majzlan *et al.*, 2005a). The chemical composition of the natural coquimbite deviates significantly from the nominal formula $Fe_2(SO_4)_3(H_2O)_9$ because of an appreciable concentration of Al on the 2*b* site (Table 4). Similar preference of Fe and Al for crystallographic sites in coquimbite was reported by Fang & Robinson (1970). The Al/(Al+Fe) ratio in the coquimbite sample is 0.225, based on chemical analysis, and 0.265, based on XRD refinement. Because the impurity phase in the coquimbite sample is unknown and may contain aluminum, preference was given to the Al/(Al+Fe) ratio calculated from XRD data. The calculated formula for rhomboclase (Table 8) indicates excess sulfuric acid, when compared to the ideal formula. Excess sulfate and protons might conceivably be stored in the interlayer portion of the rhomboclase structure. The existence of free sulfuric acid trapped between the particles in the sample is improbable for two reasons. First, the particles were large, visible by unaided eye, and carefully dried after the synthesis. Unlike powders made of small particles, this sample did not appear to be able to hold liquid in the interstices. Second, sulfuric acid dissolves in water with the release of very large amount of heat which would swamp the measured solution enthalpy. No such effect was observed. The calculated and ideal formulae for ferricopiapite (Table 8) also differ slightly. As expected (*cf.* Fanfani *et al.*, 1973), the 1*a* position in the ferricopiapite structure is not fully occupied. Similarly as for coquimbite, preference was given to wet chemical data over XRD results, when calculating the formula of ferricopiapite.

All Fe^{III} sulfates are sensitive to ambient temperature and humidity, and may be altered to a different phase when they are outside of their stability field. Because these stability fields are either unknown or known only approximately (Waller, 1992), we stored all Fe^{III} sulfates in a controlled environment (295 K, 55 % relative humidity) and checked them periodically to detect any signs of decomposition. XRD and weight loss experiments of all studied Fe^{III} sulfates were performed daily for the duration of the experiments. No changes were observed for any of the studied phases by either technique.

Thermodynamics of the reference materials

Because enthalpy has no absolute scale, the enthalpy-of-solution measurements must be performed with respect to a set of reference compounds. These compounds should be well studied, well behaved in calorimetric experiments, and easily handled. Anhydrous $Fe_2(SO_4)_3$ was not used a reference compound because of difficult handling owing to its hygroscopic nature and sluggish dissolution in acid. Sulfuric acid, used in some previous studies (*e.g.*, Ko & Daut, 1980), was not used because our calorimeter has been optimized for en-

thalpy measurements on solid samples and measurements on liquids are not currently possible. The reference compounds selected for this study are α-$MgSO_4$, MgO (periclase), γ-FeOOH (lepidocrocite), and liquid H_2O. The enthalpy of formation of MgO is well constrained by oxygen-bomb calorimetry and HCl-solution calorimetry (see Chase, 1998), and further refined by combination of thermodynamic data and numerous phase-equilibria studies (Berman, 1988). Thermochemistry of α-$MgSO_4$ was studied by Ko & Daut (1980) who, for the first time, investigated α- and β-$MgSO_4$ separately. The enthalpy of formation of lepidocrocite was measured and evaluated within the system Fe_2O_3-H_2O by Majzlan *et al.* (2003). Enthalpy of formation of liquid water has been a subject of numerous studies (Chase, 1998) and is well known. In addition, the enthalpy of water dissolution (*i.e.*, dilution) has been tabulated over a range of temperatures and HCl concentrations (van Nyus, 1943; Parker, 1965). Therefore, the enthalpy of dissolution of H_2O (*i.e.*, enthalpy of dilution) has not been measured experimentally, but was calculated from these sources.

Thermodynamics of the ferric sulfates

Enthalpy

The dissolution enthalpies of Fe^{III} sulfates and the reference phases were measured to calculate the enthalpy change of reactions 10–13 (see Table 10) *via* a thermochemical cycle. Enthalpy changes of reactions 10–13 can be calculated from experimental data (ΔH_1-ΔH_9, Table 10) using the Hess' law which states that the heat evolved or absorbed in a chemical process is the same whether the process takes place in one or in several steps. The equations for ΔH_{10}-ΔH_{13} in terms of ΔH_1-ΔH_9 are given in Table 11. Using ΔH_{10}-ΔH_{13} and the formation enthalpies of the reference phases (ΔH_{14}-ΔH_{18}, Tables 10 and 11), one may use Hess' law again to construct another set of thermochemical cycles, and to calculate the formation enthalpies of the studied Fe^{III} sulfates (ΔH_{19}-ΔH_{22}) from elements at T = 298.15 K. The corresponding equations are also listed in Table 11. The standard state of elements in this study are solid crystalline Fe, Al, and S (orthorhombic), and ideal gases O_2 and H_2.

The enthalpy of dissolution of periclase (ΔH_4) and Fe^{III} sulfates (ΔH_6-ΔH_9) was measured sequentially. A fresh batch of solvent was used to measure sequentially the dissolution enthalpy of α-$MgSO_4$ (ΔH_3) and γ-FeOOH (ΔH_2). A small amount of water, necessary to balance the equation, was added to the solvent before the dissolution of α-$MgSO_4$ and γ-FeOOH. For the experiments with coquimbite, $Al_2(SO_4)_3$ was dissolved (ΔH_5) after addition of appropriate amounts of H_2O, $MgSO_4$, and FeOOH to the solvent. The enthalpy of dilution (ΔH_1) was calculated from the tables of Parker (1965).

The uncertainties of the measured data are reported as two standard deviations of the mean, and are propagated by a standard procedure (Taylor, 1982, p. 73). If a calculated enthalpy change ΔH_{calc} is a function of m measured enthalpies ΔH_1, ΔH_2, …, ΔH_{m-1}, ΔH_m, such that

$$\Delta H_{calc} = \nu_1 \Delta H_1 + \nu_2 \Delta H_2 + \ldots + \nu_{m-1} \Delta H_{m-1} + \nu_m \Delta H_m$$

where the ν_1, ν_2, …, ν_m are the stoichiometric coefficients, then the uncertainty $\sigma(\Delta H_{calc})$ is

$$\sigma(\Delta H_{calc}) = \sqrt{[\nu_1 \sigma(\Delta H_1)]^2 + [\nu_2 \sigma(\Delta H_2)]^2 + \ldots + [\nu_{m-1} \sigma(\Delta H_{m-1})]^2 + [\nu_m \sigma(\Delta H_m)]^2}$$

where $\sigma(\Delta H_1)$, $\sigma(\Delta H_2)$, … are the uncertainties on the measured values ΔH_1, ΔH_2, …, respectively.

Table 10. Thermochemical cycle for the studied sulfates. Abbreviations: cr = crystalline solid; l = liquid; aq = aqueous species; g = gas.

reaction number	reaction
1	H_2O (l) = H_2O (aq)
2	γ-FeOOH (cr) + $3H^+$ (aq) = Fe^{3+} (aq) + $2H_2O$ (aq)
3	α-$MgSO_4$ (cr) = Mg^{2+} (aq) + SO_4^{2-} (aq)
4	MgO (cr) + $2H^+$ (aq) = Mg^{2+} (aq) + H_2O (aq)
5	$Al_2(SO_4)_3$ (cr) = $2Al^{3+}$ (aq) + $3SO_4^{2-}$ (aq)
6	$(H_3O)_{1.34}Fe(SO_4)_{2.17}(H_2O)_{3.06}$ = Fe^{3+} (aq) + $2.17SO_4^{2-}$ (aq) + $1.34H^+$ (aq) + $4.4H_2O$ (aq)
7	$Fe_2(SO_4)_3(H_2O)_{5.03}$ = $2Fe^{3+}$ (aq) + $3SO_4^{2-}$ (aq) + $5.03H_2O$ (aq)
8	$Fe_{4.78}(SO_4)_6(OH)_{2.34}(H_2O)_{20.71}$ + $2.34H^+$ = $4.78Fe^{3+}$ (aq) + $6SO_4^{2-}$ (aq) + $23.05H_2O$ (aq)
9	$Fe_{1.47}Al_{0.53}(SO_4)_3(H_2O)_{9.65}$ = $1.47Fe^{3+}$ (aq) + $0.53Al^{3+}$ (aq) + $3SO_4^{2-}$ (aq) + $9.65H_2O$ (aq)
10	$(H_3O)_{1.34}Fe(SO_4)_{2.17}(H_2O)_{3.06}$(cr) + 2.17MgO(cr) = γ-FeOOH(cr) + 2.17α-$MgSO_4$(cr) + $4.57H_2O$ (l)
11	$Fe_2(SO_4)_3(H_2O)_{5.03}$(cr) + 3MgO(cr) = 2γ-FeOOH(cr) + 3α-$MgSO_4$(cr) + $4.03H_2O$ (l)
12	$Fe_{4.78}(SO_4)_6(OH)_{2.34}(H_2O)_{20.71}$(cr) + 6MgO(cr) = 4.78γ-FeOOH(cr) + 6α-$MgSO_4$(cr) + $19.49H_2O$ (l)
13	$Fe_{1.47}Al_{0.53}(SO_4)_3(H_2O)_{9.65}$(cr) + 2.205MgO(cr) = 1.47γ-FeOOH(cr) + 2.205α-$MgSO_4$(cr) + 0.265$Al_2(SO_4)_3$(cr) + $8.915H_2O$ (l)
14	H_2 (g) + $1/2O_2$ (g) = H_2O (l)
15	Fe (cr) + O_2 (g) + $1/2H_2$ (g) = γ-FeOOH (cr)
16	Mg (cr) + S (cr) + $2O_2$ (g) = α-$MgSO_4$ (cr)
17	Mg (cr) + $1/2O_2$ (g) = MgO (cr)
18	2Al (cr) + 3S (cr) + $6O_2$ (g) = $Al_2(SO_4)_3$ (cr)
19	Fe (cr) + 2.17S (cr) + $6.54O_2$ (g) + $5.07H_2$ (g) = $(H_3O)_{1.34}Fe(SO_4)_{2.17}(H_2O)_{3.06}$ (cr)
20	2Fe (cr) + 3S (cr) + $8.515O_2$ (g) + $5.03H_2$ (g) = $Fe_2(SO_4)_3(H_2O)_{5.03}$ (cr)
21	4.78Fe (cr) + 6S (cr) + $23.525O_2$ (g) + $21.88H_2$ (g) = $Fe_{4.78}(SO_4)_6(OH)_{2.34}(H_2O)_{20.71}$ (cr)
22	1.47Fe (cr) + 0.53Al (cr) + 3S (cr) + $10.825O_2$ (g) + $9.65H_2$ (g) = $Fe_{1.47}Al_{0.53}(SO_4)_3(H_2O)_{9.65}$ (cr)

Table 11. Measured and calculated enthalpies (in kJ/mol). For reactions, refer to Table 10.

reaction enthalpy
$\Delta H_1 = \Delta H_{dilution} = -0.40$ (calculated from Parker (1965))
$\Delta H_2 = \Delta H_{dissolution(\gamma\text{-FeOOH})} = -46.15^{*} \pm 0.23^{\dagger}(10)^{\ddagger}$
$\Delta H_3 = \Delta H_{dissolution(\alpha\text{-}MgSO_4)} = -53.50 \pm 0.48(7)$
$\Delta H_4 = \Delta H_{dissolution(MgO)} = -149.68 \pm 0.60(9)$
$\Delta H_5 = \Delta H_{dissolution(Al_2(SO_4)_3)} = -232.34 \pm 2.01(7)$
$\Delta H_6 = \Delta H_{dissolution(rhomboclase)} = 15.07 \pm 0.16(7)$
$\Delta H_7 = \Delta H_{dissolution(Fe_2(SO_4)_3(H_2O)_{5.03})} = -1.79 \pm 0.45(4)$
$\Delta H_8 = \Delta H_{dissolution(ferricopiapite)} = 74.20 \pm 0.22(5)$
$\Delta H_9 = \Delta H_{dissolution(coquimbite)} = 34.58 \pm 0.58(5)$
$\Delta H_{10} = 4.57\Delta H_1 + \Delta H_2 + 2.17\Delta H_3 - 2.17\Delta H_4 - \Delta H_6 = 145.6 \pm 1.7^{\S}$
$\Delta H_{11} = 4.03\Delta H_1 + 2\Delta H_2 + 3\Delta H_3 - 3\Delta H_4 - \Delta H_7 = 196.4 \pm 2.4^{\S}$
$\Delta H_{12} = 19.49\Delta H_1 + 4.78\Delta H_2 + 6\Delta H_3 - 6\Delta H_4 - \Delta H_8 = 274.5 \pm 4.7^{\S}$
$\Delta H_{13} = 8.915\Delta H_1 + 1.47\Delta H_2 + 2.205\Delta H_3 - 2.205\Delta H_4 + 0.265\Delta H_5 - \Delta H_9 = 44.5 \pm 1.9^{\S}$
$\Delta H_{14} = \Delta H^{o}_{f(water)} = -285.8 \pm 0.1$ (Robie & Hemingway, 1995)
$\Delta H_{15} = \Delta H^{o}_{f(\gamma\text{-FeOOH})} = -549.4 \pm 1.4$ (Majzlan *et al.*, 2003)
$\Delta H_{16} = \Delta H^{o}_{f(\alpha\text{-}MgSO_4)} = -1288.8 \pm 0.5$ (DeKock, 1986)
$\Delta H_{17} = \Delta H^{o}_{f(MgO)} = -601.6 \pm 0.3$ (Robie & Hemingway, 1995)
$\Delta H_{18} = \Delta H^{o}_{f(Al_2(SO_4)_3)} = -3441.8 \pm 1.8$ (Robie & Hemingway, 1995)
$\Delta H_{19} = \Delta H^{o}_{f(rhomboclase)} = \Delta H_{10} + 4.57\Delta H_{14} + \Delta H_{15} + 2.17\Delta H_{16} - 2.17\Delta H_{17} = -3201.1 \pm 2.6^{\S}$
$\Delta H_{20} = \Delta H^{o}_{f(Fe_2(SO_4)_3(H_2O)_{5.03})} = \Delta H_{11} + 4.03\Delta H_{14} + 2\Delta H_{15} + 3\Delta H_{16} - 3\Delta H_{17} = -4115.8 \pm 4.1^{\S}$
$\Delta H_{21} = \Delta H^{o}_{f(ferricopiapite)} = \Delta H_{12} + 19.49\Delta H_{14} + 4.78\Delta H_{15} + 6\Delta H_{16} - 6\Delta H_{17} = -12045.1 \pm 9.2^{\S}$
$\Delta H_{22} = \Delta H^{o}_{f(coquimbite)} = \Delta H_{13} + 8.915\Delta H_{14} + 1.47\Delta H_{15} + 2.205\Delta H_{16} - 2.205\Delta H_{17} + 0.265\Delta H_{18} = -5738.4 \pm 3.3^{\S}$

* mean
† two standard deviations of the mean
‡ number of measurements
§ error propagated as described by Taylor (1982; see text)

Entropy

Entropy is a thermodynamic quantity that has been estimated in a number of studies with much greater success than enthalpy (see Nordstrom & Munoz, 1994, p. 352–357). Since entropy of the investigated Fe^{III} sulfates has not been measured, we had to estimate the values. The simplest method for entropy estimation is expressed by the equation

$$S = \Sigma \nu_i S_i \quad (1)$$

meaning that the entropy to be determined (S) is a simple sum of entropies of suitably chosen components (S_i) (Latimer, 1952). The variable ν_i is the stoichiometric coefficient of the component i. The selected components may be elements, ions, oxides, or more complicated chemical entities. The method was later modified by Fyfe *et al.* (1958) to

$$S = \Sigma \nu_i S_i + k(V - \Sigma \nu_i V_i) \quad (2)$$

where V is the molar volume of the phase whose entropy is to be determined and V_i's are the molar volumes of the components. The modification aims to account for the volume changes between the phase whose entropy is being estimated and the sum of the components. Holland (1989) used eq. (2) to review entropy data for a number of silicates and to determine the value of $k = 1.00$.

Table 12. Components used in estimation of entropy (see text). Entropy of MgO, $MgSO_4$, $Mg(OH)_2$, and $Al_2(SO_4)_3$ taken from Robie & Hemingway (1995). Entropy of $Fe_2(SO_4)_3$ taken from Majzlan *et al.* (2005b). Molar volume of $Mg(OH)_2$ from Robie & Hemingway (1995); those of MgO, $MgSO_4$, and $Al_2(SO_4)_3$ calculated from the structural data in Table 1; that of $Fe_2(SO_4)_3$ from Majzlan *et al.* (2005b).

component	S^o (J/mol·K)	V^o (cm^3/mol)
MgO	26.9±0.2	11.24
$Mg(OH)_2$	63.2±0.1	24.63
$MgSO_4$	91.4±0.8	39.75
$Fe_2(SO_4)_3$	305.6±0.6	123.94
$Al_2(SO_4)_3$	239.2±1.2	119.90

The components chosen for entropy estimation procedure in this study are listed in Table 12. The stoichiometric coefficients ν_i are in Table 13. The component $Fe_2(SO_4)_3$ was chosen because

(1) the coordination of Fe and S in $Fe_2(SO_4)_3$ are identical to those in the studied Fe^{III} sulfates. Holland (1989) showed that an ionic component (*e.g.*, Fe^{III}) should be assigned different entropy values if it occurs in variable coordination environment. Therefore, a choice of component with identical coordination geometries for all ions is important.

(2) in addition to the vibrational (lattice) entropy, this component accounts fully for the magnetic entropy of all studied Fe^{III} sulfates. The number of Fe^{III} ions in the $Fe_2(SO_4)_3$ component and the Fe^{III} sulfates is precisely matched (see Table 13).

The components MgO, $Mg(OH)_2$, and $MgSO_4$ were chosen because

(1) they can account for H_2O and possible excess (SO_4) groups that cannot be matched by the $Fe_2(SO_4)_3$ component. These components are much more suitable than oxide components H_2O and SO_3. Both H_2O and SO_3 are fictive components, as they are not solids at $T = 298.15$ K, and their entropy and volume would have to be estimated first. Such a procedure (for H_2O) has been presented for silicates by Holland (1989) who, however, noticed that "H_2O was the most difficult parameter to define". The significantly smaller database for sulfates makes us question the validity of any entropy and volume estimates for the fictive H_2O and SO_3 components.

(2) Mg^{II} in all three components is in identical (octahedral) coordination, and therefore can be cancelled out without any additional corrections.

The component $Al_2(SO_4)_3$ was chosen because the octahedral coordination of Al^{III} and tetrahedral coordination in the sulfate molecule match the coordination geometries in coquimbite.

Entropy values estimated using both equation 1 and 2 are given in Table 14. Because the value of $k = 1.00$ was estimated by regression on data determined for silicates (Holland, 1989), the following text and calculations use the entropy values estimating by equation 1.

Stability of Fe^{III} sulfates

The measured formation enthalpy, estimated entropy, and calculated Gibbs free energy for the studied sulfates are summarized in Table 14. These values can be used to calculate phase diagrams and to predict the existence or absence of these minerals in natural assemblages at specified conditions. However, such calculations are difficult at the moment because available data on other Fe-sulfate phases remain too sparse and models of concentrated aqueous solutions are incomplete. Measured thermodynamic values for the Fe^{III} sulfate minerals are limited to those presented in this study and jarosite group minerals (Stoffregen, 1993; Baron & Palmer, 1996; Majzlan *et al.*, 2004). Jerz & Rimstidt (2003) constructed approximate phase diagram for a paragenesis of Fe^{II}-Fe^{III} sulfates and oxides based on field observations. Paragenetic relationships among Fe sulfates at Iron Mountain have been described by Alpers *et al.* (1994, 2003), Nordstrom & Alpers (1999b), and Jambor *et al.* (2000). Jamieson *et al.* (2005) determined that magnesiocopiapite is stable at lower pH than hydronium jarosite, based on stoichiometry and field relations. Thermodynamics of the hydrated Fe^{II} sulfates have been studied in greater detail than the Fe^{III} sulfates (Parker & Khodakovskii, 1995; Chou *et al.*, 2002). The phase equilibria among the Fe^{III} sulfates and coexisting solutions are not well established. At room temperature, Baskerville & Cameron (1935) approximately delineated the stability fields of ferricopiapite, rhomboclase, and probably also kornelite and coquimbite. Posnjak & Merwin (1922) presented the results of similar investigations at temperatures ≥323 K, and Merwin & Posnjak (1937) estimated the phase relationships at 303–313 K based on field observations. The sequence of stability of Fe^{III} sulfates with an increasing component of sulfuric acid at 323 K can be inferred from the phase diagram of Posnjak & Merwin (1922). The sequence is goethite – hydronium jarosite – butlerite – ferricopiapite – kornelite – rhomboclase – $(H_3O)Fe(SO_4)_2$. Activity of water and mean activity coefficients for $Fe_2(SO_4)_3$ have been measured in a range of $Fe_2(SO_4)_3$–H_2SO_4–H_2O solutions (Majima & Awakura, 1985, 1986). Specific ion interaction (Pitzer) model coefficients are available for the Fe^{II}-SO_4 solutions (Reardon & Beckie, 1987; Pitzer, 1991), and similar work for the Fe^{III}-SO_4 solutions has appeared only recently (Christov, 2004; Rumyantsev *et al.*, 2004).

A phase diagram based on the data presented in this contribution is shown in Fig. 1. The presented phase diagram should be considered only as preliminary and schematic because the aqueous speciation is such concentrated solutions could not be taken fully into account. Namely, the problem is the position of the predominance boundary of the $(SO_4)^{2-}$–$(HSO_4)^-$. Dickson *et al.* (1990) showed that the two sulfur-bearing species occur at equal concentrations in concentrated solutions at T = 298.15 K at pH ~1. However, unless the position of the boundary is known precisely, and the activity coefficients of both species can be calculated, the phase diagram will show discontinuities at the arbitrarily selected predominance boundary. Therefore, the entire diagram (Fig. 1) is calculated with $(SO_4)^{2-}$ as the only aqueous sulfur-bearing species. Assuming the predominance boundary at pH = 1, the boundaries of the stability fields for ferricopiapite-hydronium jarosite (pH = 1.06) and hydronium jarosite-goethite (pH = 1.60) are the stable boundaries for the activities of sulfate and water specified in Fig. 1. However, the boundary between ferricopiapite-rhomboclase (pH = –0.05) is metastable. If the boundary is calculated for HSO_4^- as the predominant species, assuming that $a_{SO42-} = a_{HSO4-}$, it will shift to pH = –2.08. All boundaries that lie left to the selected (SO_4^{2-})-HSO_4^- predominance boundary at pH = 1 are then metastable extensions from the field of SO_4^{2-} predominance into the field of HSO_4^- predominance. This phase diagram certainly can be, and will be, improved as more thermodynamic data become available and additional complexity is included into its construction.

Table 13. Stoichiometric coefficients (ν_i's in equations 1 and 2) for components for estimation of entropy for Fe^{III} sulfates. The formulae of rhomboclase, ferricopiapite, and coquimbite are given in Table 8.

component	rhomboclase	$Fe_2(SO_4)_3(H_2O)_{5.03}$	ferricopiapite	coquimbite
MgO	–5.74	–5.03	–20.71	–9.65
$Mg(OH)_2$	+5.07	+5.03	+21.88	+9.65
$MgSO_4$	+0.67	0	–1.17	0
$Fe_2(SO_4)_3$	+0.50	+1.00	+2.39	+0.735
$Al_2(SO_4)_3$	0	0	0	+0.265

Table 14. Summary of thermodynamic properties of the studied Fe sulfate samples. The formulae of rhomboclase, ferricopiapite, and coquimbite are given in Table 5. All thermodynamic quantities are given per one mole of the composition in Table 8.

quantity/phase	$Fe_2(SO_4)_3(H_2O)_{5.03}$	coquimbite	ferricopiapite	rhomboclase
ΔH^o_f (kJ/mol)	–4115.8±4.1	–5738.4±3.3	–12045.1±9.2	–3201.1±2.6
S^o (J/mol·K)*	488.2	638.3	1449.2	380.1
S^o (J/mol·K)†	493.6	651.5	1468.2	376.3
ΔS^o_f (J/mol·K)‡	–2066.3	–2994.5	–6558.0	–1720.8
ΔG^o_f (kJ/mol)‡	–3499.7±4.2	–4845.6±3.3	–10089.8±9.3	–2688.0±2.7
V^o (cm^3/mol)	196.72	265.32	574.84	145.24

* estimated from equation 1 and data in Tables 9 and 10

† estimated from equation 2 and data in Tables 9 and 10

‡ calculated with entropy values estimated from equation 1

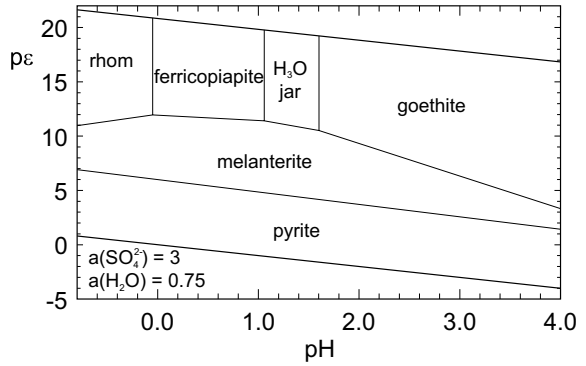

Fig. 1. Phase diagram showing the stability fields of some Fe^{III} and Fe^{II} sulfates and pyrite as a function of pH and pε. Abbreviations of phases: rhom = rhomboclase, H_3O jar = hydronium jarosite. Thermodynamic data for hydronium jarosite taken from Majzlan *et al.* (2004); those for goethite from Majzlan *et al.* (2003); those for melanterite from Parker & Khodakovskii (1995), those for pyrite from Robie & Hemingway (1995), those for $(SO_4)^{2-}$ from Nordstrom & Munoz (1994). Limitations of this phase diagrams are discussed in the text.

Despite the limitations outlined above, and other limitations of pε-pH diagrams (see Nordstrom & Munoz, 1994), the order of stability of ferric sulfate minerals with decreasing pH (hydronium jarosite, ferricopiapite, and rhomboclase, see Fig. 1) agrees with the order determined experimentally by Posnjak & Merwin (1922) and Baskerville & Cameron (1935). The diagram is also in agreement with field observations of Nordstrom & Alpers (1999b) who found rhomboclase coexisting with fluids with pH of –2.5 and –3.6, albeit at slightly elevated temperatures (315–319 K) and high concentration of metals other than Fe. Jamieson *et al.* (2005) determined the pH of fluid coexisting with magnesiocopiapite as –0.9; no data are available regarding the pH of aqueous solution coexisting with ferricopiapite.

Our current thermodynamic description of concentrated acid mine drainage systems and associated efflorescent sulfate salts is fragmentary at best, and more work is needed to fill the gaps and combine the known information into a comprehensive model. The future steps, which could significantly aid the understanding of these systems from a thermodynamic point of view, include experimental determination of enthalpies and entropies for additional sulfates, combination of such data with the ion-interaction models for Fe^{II}–Fe^{III}–SO_4, and comparison of the phase diagrams with experimental syntheses and field observations. Work along these lines is in progress.

Acknowledgements: We thank R. Angel, J. Pope, R. Peterson, R. Seal, and R. Stoffregen for constructive criticism that helped to improve the manuscript, and R. Altherr for the editorial handling of the manuscript. J.M. is grateful for the support that came from the Hess post-doctoral fellowship at the Department of Geosciences at Princeton University. We thank S.V. Ushakov for the EDS analyses of firing products, and C. Botez and P. Stephens for the help with synchrotron XRD experiments. R.B.M. and C.N.A. are grateful to the U.S. Environmental Protection Agency for providing access to the Richmond mine at Iron Mountain and funding for mineralogical and geochemical studies. The synthesis and calorimetry at UC Davis was supported by the U.S. Department of Energy (grant DE FG03 97 ER14749). This research was carried out in part at the National Synchrotron Light Source at Brookhaven National Laboratory, which is supported by the US Department of Energy, Division of Materials Sciences and Division of Chemical Sciences. The SUNY X3 beamline at NSLS was previously supported by the Division of Basic Energy Sciences of the US Department of Energy under Grant No. DE-FG02-86ER45231.

References

Alpers, C.N., Blowes, D.W., Nordstrom, D.K., Jambor, J.L. (1994): Secondary minerals and acid mine-water chemistry. *in* "Environmental Geochemistry of Sulfide Mine-Wastes", J.L. Jambor & D.W. Blowes, eds. *Mineral. Assoc. Canada, Short-Course Notes,* **22**, 247-270.

Alpers, C.N., Nordstrom, D.K., Spitzley, J. (2003): Extreme acid mine drainage from a pyritic massive sulfide deposit: The Iron Mountain end-member. *in* "Environmental Aspects of Mine Wastes", J.L. Jambor, D.W. Blowes, A.I.M. Ritchie, eds. *Mineral. Assoc. Canada, Short-Course Notes,* **31**, 407-430.

Baron, D. & Palmer, C.D. (1996): Solubility of jarosite at 4 – 35 °C. *Geochim. Cosmochim. Acta,* **60**, 185-195.

Baskerville, W.H. & Cameron, F.K. (1935): Ferric oxide and aqueous sulfuric acid at 25 °C. *J. Phys. Chem.,* **39**, 769-779.

Berman, R.G. (1988): Internally consistent thermodynamic data for minerals in the system Na_2O-K_2O-CaO-MgO-FeO-Fe_2O_3-Al_2O_3-SiO_2-TiO_2-H_2O-CO_2. *J. Petrol.,* **29**, 445-522.

Chase, M.W., Jr. (ed.) (1998): NIST-JANAF thermochemical tables. Fourth Edition. *J. Phys. Chem. Ref. Data*, monograph no. **9**, 1538.

Chou, I.-M., Seal, R.R., II, Hemingway, B.S. (2002): Determination of melanterite-rozenite and chalcanthite-bonattite equilibria by humidity measurements at 0.1 MPa. *Am. Mineral.,* **87**, 108-114.

Christensen, H. & Christensen, A.N. (1978): Hydrogen bonds of γ-FeOOH. *Acta Chem. Scand., Series A,* **32**, 87-88.

Christov, C. (2004): Pitzer ion-interaction parameters for Fe(II) and Fe(III) in the quinary {Na + K + Mg+ Cl + SO_4 + H_2O} system at T = 298.15 K. *J. Chem. Thermodyn.,* **36**, 223-235.

Cravotta, C.A., III (1994): Secondary iron-sulfate minerals as sources of sulfate and acidity: Geochemical evaluation of acidic groundwater at a reclaimed surface coal mine in Pennsylvania. *in* "Environmental geochemistry of sulfide oxidation", C.N. Alpers & D.W. Blowes, eds. *Am. Chem. Soc. Symp. Ser.,* **550**, 345-364.

Dahmen, T. & Gruehn, R. (1993): Beiträge zum thermischen Verhalten von Sulfaten. IX. Einkristallstrukturverfeinerung der Metall(III)-sulfate $Cr_2(SO_4)_3$ und $Al_2(SO_4)_3$. *Z. Kristallogr.,* **204**, 57-65.

DeKock, C.W. (1986): Thermodynamic properties of selected metal sulfates and their hydrates. *U.S. Bur. Mines, Inform. Circ.,* **9081**.

Dickson, A.G., Wesolowski, D.J., Palmer, D.A., Mesmer, R.E. (1990): Dissociation constant of bisulfate ion in aqueous sodium chloride solutions to 250 °C. *J. Phys. Chem.,* **94**, 7978-7985.

Fanfani, L., Nunzi, A., Zanazzi, P.F., Zanzari, A.R. (1973): The copiapite problem: The crystal structure of a ferrian copiapite. *Am. Mineral.,* **58**, 314-322.

Fang, J.H. & Robinson, P.D. (1970): Crystal structures and mineral chemistry of hydrated ferric sulfates. I. The crystal structure of coquimbite. *Am. Mineral.,* **55**, 1534-1540.

Finger, L.W., Cox, D.E., Jephcoat, A.P. (1994): A correction for powder diffraction peak asymmetry due to axial divergence. *J. Appl. Crystallogr.,* **27**, 892-900.

Fyfe, W.S., Turner, F.J., Verhoogen, J. (1958): Metamorphic reactions and metamorphic facies. *Geol. Soc. Am. Memoir,* **75**, 253 pp.

Hemingway, B.S., Seal. R.R., II, Chou, I.-M. (2002): Thermodynamic data for modeling acid mine drainage problems: Compilation and estimation of data for selected soluble iron-sulfate minerals. *U.S. Geol. Survey, Open-File Report,* **02-161**, 13 pp.

Holland, T.J.B. (1989): Dependence of entropy on volume for silicate and oxide minerals: A review and predictive model. *Am. Mineral.,* **74**, 5-13.

Jambor, J.L. (2003): Mine-waste mineralogy and mineralogical perspectives of acid – base accounting. *in* "Environmental Aspects of Mine Wastes", J.L. Jambor, D.W. Blowes, A.I.M. Ritchie, eds. *Mineral. Assoc. Canada, Short-Course Notes,* **31**, 117-145.

Jambor, J.L, Nordstrom, D.K., Alpers, C.N. (2000): Metal-sulfate salts from sulfide mineral oxidation. *in* "Sulfate Minerals: Crystallography, Geochemistry, and Environmental Significance", C.N. Alpers, J.L. Jambor, D.K. Nordstrom, eds. *Rev. Mineral. Geochem.,* **40**, 303-350.

Jamieson, H.E., Robinson C., Alpers, C.N., McCleskey, R.B., Nordstrom, D.K., Peterson, R.C. (2005): Major and trace element composition of copiapite-group minerals and coexisting water from the Richmond Mine, Iron Mountain, California. *Chemical Geol.,* **215**, 387-405.

Jerz, J.K. & Rimstidt, J.D. (2003): Efflorescent iron sulfate minerals; paragenesis, relative stability, and environmental impact. *Am. Mineral.,* **88**, 1919-1932.

Ko, H.C. & Daut, G.E. (1980): Enthalpies of formation of α- and β-magnesium sulfate and magnesium sulfate monohydrate. *U.S. Bur. Mines Rep. Invest.,* **8409**.

Larson, A.C. & von Dreele, R.B. (1994): GSAS. General Structure Analysis System. LANSCE, MS-H805, Los Alamos, New Mexico.

Latimer, W.L. (1952): Oxidation potentials. 2nd edition. Prentice-Hall.

Majima, H. & Awakura, Y. (1985): Water and solute activities of H_2SO_4-$Fe_2(SO_4)_3$-H_2O and HCl-$FeCl_3$-H_2O solution systems. Part I. Activities of water. *Metall. Trans. B,* **16**, 433-439.

–,– (1986): Water and solute activities of H_2SO_4-$Fe_2(SO_4)_3$-H_2O and HCl-$FeCl_3$-H_2O solution systems. Part II. Activities of solutes. *Metall. Trans. B,* **17**, 621-627.

Majzlan, J. & Kiefer, B. (2006): An X-ray and neutron diffraction and *ab-initio* study of the crystal structure of ferricopiapite, $Fe_{14/3}(SO_4)_6(OH)_2(H_2O)_{20}$. *Can. Mineral.* (submitted)

Majzlan, J., Grevel, K.-D., Navrotsky, A. (2003): Thermodynamics of iron oxides: Part II. Enthalpies of formation and relative stability of goethite (α-FeOOH), lepidocrocite (γ-FeOOH), and maghemite (γ-Fe_2O_3). *Am. Mineral.,* **88**, 855-859.

Majzlan, J., Stevens, R., Boerio-Goates, J., Woodfield, B.F., Navrotsky, A., Crawford, M., Burns, P., Amos, T.G. (2004): Thermodynamic properties, low-temperature heat capacity anomalies, and single crystal X-ray refinement of hydronium jarosite, $(H_3O)Fe_3(SO_4)_2(OH)_6$. *Phys. Chem. Minerals,* **31**, 518-531.

Majzlan, J., Botez, C., Stephens, P.W. (2005a): The crystal structures of synthetic $Fe_2(SO_4)_3(H_2O)_5$ and the type specimen of lausenite. *Am. Mineral.,* **90**, 411-416.

Majzlan, J., Stevens, R., Donaldson, M., Boerio-Goates, J., Woodfield, B.F., Navrotsky, A. (2005b): Thermodynamics of monoclinic $Fe_2(SO_4)_3$. *J. Chem. Thermodyn.,* **37**, 802-809.

Mereiter, K. (1974): Die Kristallstruktur von Rhomboklas $(H_5O_2)^+(Fe(SO_4)_2(H_2O)_2)$. *Tscher. Miner. Petrog.,* **21**, 216-232.

Merwin, H.E. & Posnjak, E. (1937): Sulphate incrustations in the copper Queen mine, Bisbee, Arizona. *Am. Mineral.,* **22**, 567-571.

Nordstrom, D.K. & Alpers, C.N. (1999a): Geochemistry of acid mine waters. *in* "The Environmental Geochemistry of Mineral Deposits. Part A: Processes, Methods, and Health Issues", G.S. Plumlee & M.J. Logsdon, eds. *Rev. Econ. Geol.,* **6A**, 133-160.

–,– (1999b): Negative pH, efflorescent mineralogy, and consequences for environmental restoration at the Iron Mountain Superfund site, California. *Proc. Nat. Acad. Sci. USA,* **96**, 3455-3462.

Nordstrom, D.K. & Munoz, J.L. (1994): Geochemical Thermodynamics. 2nd edition, Blackwell Scientific Publications.

Parker, V.B. (1965): Thermal properties of uni-univalent electrolytes. *Natl. Stand. Ref. Data Series, Natl. Bur. Stand.,* **2**, 66 pp.

Parker, V.B. & Khodakovskii, I.L. (1995): Thermodynamic properties of the aqueous ions (2+ and 3+) of iron and they compounds of iron. *J. Phys. Chem. Ref. Data,* **24**, 1669-1745.

Pitzer, K.S. (1991): Ion interaction approach: Theory and data collection. *in* "Activity Coefficients in Electrolyte Solutions" K.S. Pitzer, ed. 1. CRS, Boca Raton, 75-153.

Posnjak, E. & Merwin, H.E. (1922): The system, $Fe_2O_3 – SO_3 – H_2O$. *J. Am. Chem. Soc.,* **44**, 1965-1994.

Ptacek, C. & Blowes, D. (2000): Predicting sulfate-mineral solubility in concentrated waters. *in* "Sulfate Minerals: Crystallography, Geochemistry, and Environmental Significance" C.N. Alpers, J.L. Jambor, D.K. Nordstrom, eds. *Rev. Mineral. Geochem.,* **40**, 513-540.

Reardon, E.J. & Beckie, R.D. (1987): Modelling chemical equilibria of acid-mine drainage: The $FeSO_4$-H_2SO_4-H_2O system. *Geochim. Cosmochim. Acta,* **51**, 2355-2368.

Rentzeperis, P.J. & Soldatos, C.T. (1992): The crystal structure of the anhydrous magnesium sulfate. *Acta Crystallogr.,* **11**, 686-688.

Robie, R.A. & Hemingway, B.S. (1995): Thermodynamic properties of minerals and related substances at 298.15 K and 1 bar (10^5 Pascals) and at higher temperatures. *U.S. Geol. Survey Bull.,* **2131**, 461 pp.

Rumyantsev, A.V., Hagemann, S., Moog, H.C. (2004): Isopiestic investigation of the systems $Fe_2(SO_4)_3$-H_2SO_4-H_2O, $FeCl_3$-H_2O, and Fe(III)-(Na, K, Mg, Ca)Cl_n-H_2O at 298.15 K. *Z. Phys. Chem.,* **218**, 1089-1127.

Stoffregen, R.E. (1993): Stability relations of jarosite and natrojarosite at 150-250 °C. *Geochim. Cosmochim. Acta,* **57**, 2417-2429.

Stookey, L.L. (1970): Ferrozine – A new spectrophotometric reagent for iron. *Anal. Chem.,* **42**, 779-781.

Taylor, J.R. (1982): An Introduction to Error Analysis. The Study of Uncertainties in Physical Measurements. Oxford University Press.

Tsirelson, V.G., Avilov, A.S., Abramov, Yu.A., Belokoneva, E.L., Kitaneh, R., Feil, D. (1998): X-ray and electron diffraction study of MgO. *Acta Crystallogr., B* **54**, 8-17.

Young, J.E. (1992): Mining the earth: Worldwatch Institute, Worldwatch Paper **109**, 53 pp.

Young, R.A. (1993): Introduction to the Rietveld method. *in* "The Rietveld Method", R.A. Young, ed. International Union of Crystallography monograph 5, 1-38.

van Nuys, C.C. (1943): Enthalpy and heats of dilution of the system HCl-H_2O. *Trans. Am. Inst. Chem. Eng.,* **39**, 663-678.

Waller, R. (1992): Temperature- and humidity-sensitive mineralogical and petrological specimens. *in* "The Care and Conservation of Geological Material: Minerals, Rocks, Meteorites and Lunar Finds", F.M. Howie, ed. Butterworth – Heinemann, 25-50.

Received 20 January 2005
Modified version received 10 August 2005
Accepted 14 October 2005